Effect of SiC and B_4C Reinforcements on the Structural and Mechanical Properties of Aluminum Composites Fabricated by Spark Plasma Sintering

Shaafi T
Department of Mechanical Engineering, Saveetha School of Engineering, Saveetha Institute of Medical and Technical Sciences

Kalaimani M
Department of Mechanical Engineering, Excel Engineering College, Komarapalayam, Namakkal

Karthick S
Department of Mechanical Engineering, Excel Engineering College, Komarapalayam

Senthilkumar N
Department of Mechanical Engineering, Ganesh College of Engineering

https://doi.org/10.5109/7363512

出版情報：Evergreen. 12 (2), pp.1322-1335, 2025-06. Transdiscilinary Research and Education Center for Green Technologies, Kyushu University
バージョン：

Effect of SiC and B_4C Reinforcements on the Structural and Mechanical Properties of Aluminum Composites Fabricated by Spark Plasma Sintering

T. Shaafi[1], M. Kalaimani[1,*], S. Karthick[2], N. Senthilkumar[3]

[1]Department of Mechanical Engineering, Saveetha School of Engineering, Saveetha Institute of Medical and Technical Sciences, Chennai, India
[2]Department of Mechanical Engineering, Excel Engineering College, Komarapalayam, Namakkal, India
[3]Department of Mechanical Engineering, Ganesh College of Engineering, Salem, India

*Author to whom correspondence should be addressed:
E-mail: kalaimanim9062.sse@saveetha.com

(Received January 30, 2025; Revised May 30, 2025; Accepted June 04, 2025)

Abstract: Aluminum composites have been used for their low weight, more effective wear resistance, and suitability for high-strength purposes. It is capable of enduring the challenging environments commonly encountered in automotive and aerospace applications. The spark plasma sintering (SPS) methods, conducted at 550 °C, enhanced the aluminum matrix with ceramic particles of SiC and B_4C at varying weight percentages of 5, 10, and 15 wt.%, resulting in distinct aluminum composites, such as Al/SiC and Al/B_4C composite. In the SPS method, particle size and densification range are the primary reasons for the increase in porosity, which affects the grain structure and mechanical characteristics of the aluminum composite. The study evaluated the composite's material grain structure, density, and mechanical properties. It has been noted that the mechanical properties change and the type of reinforcement used within specific limits. Aluminum composites reinforced with ceramics exhibit improved mechanical strength. At 15 wt.% reinforcement, Al/B_4C had the maximum microhardness (88 Hv), which was higher than Al/SiC (80 Hv) with the same, brittleness occurred upward. At 10 wt.%, the highest tensile strength was reached, with Al/B_4C-210.56 MPa and Al/SiC-194.37 MPa. The material's brittleness was demonstrated by Al/B_4C, which exhibited an elongation of 8.76%, and Al/SiC was 8.97%. This indicates that the material was brittle. At 10 wt.%, Al/SiC had a greater compressive strength (257 MPa) than Al/B_4C (252 MPa). The mechanical properties of both composites were greatest when 10 wt.% reinforcement was added.

Keywords: aluminum composite; structural property; mechanical property; spark plasma sintering

1. Introduction

Structural components commonly use aluminum metal matrix due to its high load-carrying capacity, low density, and good conductivity. Scientists have created various materials to address this challenge, notably the composite metal matrix (MMC). AMC is widely utilized in many applications owing to its notable characteristics. These Include minimal density, substantial strength, excellent stiffness, durability against corrosion, low shock resistance to heat, and enhanced mechanical propertie[1,2)]. Widely applicable, MMC is used in many industries, including aerospace[3)], transportation[4)], defence[5)], and maritime[6)]. AMC is an aluminum matrix composite material reinforced with ceramic, fiber, and whisker particles[7)]. Particulate material composites have several benefits. By giving the matrix material reinforcement, they strengthen the material. Combining reinforcement can achieve specific material characteristics. Particles dissolved in a matrix, such as metals and ceramics, comprise particulate composite materials. As a result of the stochastic introduction of particles, they are typically isotropic[8)]. Particulate composites offer several benefits, including enhanced oxidation resistance, higher working temperatures, and greater strength[9,10)]. The reinforcements of hard ceramic particles such as SiC[11)], TiC[12)], TiO_2[13)], ZrO_2[14)], ZrB_2[15)], Al_2O_3[16)], B_4C[17)] and TiB_2[18)] are used as a common reinforcement particle in the aluminum matrix

Cite: S. T et al., "Effect of SiC and B·C Reinforcements on the Structural and Mechanical Properties of Aluminum Composites Fabricated by Spark Plasma Sintering". Evergreen, 12 (02) 1322-1335 (2025). https://doi.org/10.5109/7363512.

composites. Among these ceramic reinforcements, the most desirable mechanical, wear, and thermal properties of aluminum composite materials are achieved by silicon carbide (SiC) and boron carbide (B_4C). High modulus and strength characterize the most frequently employed particulates, including carbides, oxides, and nitrides. SiC is chemically inert, has a small thermal expansion, and exhibits superior abrasion resistance and oxidation resistance at elevated temperatures, in addition to its high thermal conductivity and stability. Furthermore, its density is similar to that of aluminum, contributing to the isotropic characteristics exhibited by Al/SiC composites[19]. The progressive role interacting process produces the Al/SiC composite. Najjar et al.[20] investigated the physical properties of tensile characteristic of 254 MPa, yield properties of 230 MPa, and hardness of 76.5 HV was the ninth roll pass in the bounding process at the 4 wt.% of SiC developed by the machine learning approach. The effect of SiC reinforced with aluminum with varying reinforcement levels. SiC increased impact resistance but also produced greater cracking and breaking at higher fractions. Composite samples outperformed unreinforced samples in impact testing[21]. The composites were produced using the incorporation of SiO_2 reinforcement, which enhances the mechanical attributes of the composites. The morphology and physical properties of the produced metal matrix composites were evaluated. The mechanical properties, such as tensile strength, hardness, and impact resistance, have shown improvement relative to those of unreinforced alloy[22]. Chintada et al.[23] stated that the Al-5wt.%SiC composite material fabricated by the microwave sintering technique has increased mechanical properties and decreased density, porosity, and elongation properties compared to the aluminum material. Experimental assessments of aluminum matrix composites strengthened using silicon nitride (Si_3N_4) particles have been performed to assess their microhardness, compressive strength, impact resistance, tensile strength, wear resistance, and corrosion resistance, following ASTM standards[24]. Alam et al.[25] reported that the composites with a SiC content of 7.5 weight percent and a sintering temperature of 550°C have the maximum Vickers hardness, measuring 59.68 VHN. Since the reinforcing element aggregates at the matrix particle interface, further SiC inclusion reduces the composite's hardness. Leszczyńska et al.[26] claimed that morphological and tribological attributes of Al–SiC composites developed through the SPS process. Composites with a substantial SiC particles presence (90wt%) demonstrated enhanced hardness 2537HV and bending strength 242MPa, accompanied by a reduction in wear resistance. Under a friction load of 100N, the wear loss was 0.43%, while at a friction load of 200N, the wear loss increased to 0.76%. The values were significantly elevated in comparison to the composites containing a reduced SiC phase (70 wt%), exhibiting weight losses that were 360% and 270% greater, respectively. These values were significantly higher compared to the composites containing a minimal SiC phase content (70wt%), with weight losses of 360% and 270% higher, respectively. The wear rate exhibited a significant increase in the Al-SiC with 90 wt% composites, reaching three times the rate observed in other materials.

Utilizing the hot-pressing method, solid-state powder metallurgy was used to create aluminum matrix composites reinforced with boron carbide (B_4C) varying in weight from 2 to 12 wt.%. Brillon et al.[27] observed that B_4C particles reduced the ductility and raised the composite material's hardness and strain hardening threshold to 85% and 55%, respectively, up to 12% in the Al matrix. It was measured that the mechanical characteristics rise to up to 8 vol.% B_4C while the elongation at rupture decreases. Al/B_4C gets more brittle at more significant B_4C volume fractions, which results in a limited number of plastic phases. Gou et al.[28] Hot pressing sintering successfully produced B_4C/Al composites. Al_3BC was identified as the component of B_4C/Al composites, despite the sintered process at a relatively minimal temperature of 570 °C. The presence of Al_3BC nanoparticles within the Al matrix results in a notable enhancement in strength, the strength is approximately 65 MPa, attained via geometrically necessary dislocation resistance, and Orowan enhancing is implemented in composites that contain B_4C particles at 30wt.%. This paper presents an analysis of Al_3BC synthesis and its role in enhancing strength, along with the mechanisms involved in this strengthening process. Dwivedi et al.[17] fabricated an AA2014 aluminum matrix reinforced by B_4C and synthesized by stir casting. It was noticed that 10 wt.% of B_4C increased the tensile strength to 235 MPa and hardened it to 98 BHN, and it was stated that hardness increased, while ductility and toughness decreased. Pehlivanlı et al.[29], using a powder metallurgy process, created composite materials at sintering by varying temperatures by different wt.% of reinforcement of B_4C to Al 1070 grade aluminum. The maximum heat conduction coefficient was achieved at a 600°C sintering temperature and a 4% B_4C reinforcement ratio. The authors noted that they accurately calculated the thermal conductivity coefficient using the experimental findings and the FEA models. The synthesized composites exhibit a consistent increase in strength under compression (24%) and hardness (14%) compared to the base alloy. The ASTM B117, test for salt precipitation was conducted to examine the corrosion characteristics of the incorporated composites[30]. Ozay et al.[31] This study employed hot press sintering to apply a coating of an Al/B_4C reinforced composite onto the exterior of the AA-2024 aluminum alloy. Pure Al powder has been applied to the AA-2024 material under a pressure of 110 MPa. Metal matrix composites containing A l5 wt.% B_4C were deposited on

Cite: S. T et al., "Effect of SiC and B·C Reinforcements on the Structural and Mechanical Properties of Aluminum Composites Fabricated by Spark Plasma Sintering". Evergreen, 12 (02) 1322-1335 (2025). https://doi.org/10.5109/7363512.

the AA-2024 substrate in the other samples at 90, 110, and 130 MPa. Additionally, the size and gaps between the grains in the coating layer's microstructure shrank as the pressing pressure increased. It was therefore shown that weight loss decreased and microhardness increased. This article examines various nano reinforcements, their impacts, and suitable processing techniques for aluminum and its alloys to identify the least effective reinforcement mixtures for hybrid composites[32]. Gaylan et al.[33] reported that aluminum was reinforced with B_4C (5 to 50wt.%) with cold compaction of 500 MPa and sintered at 600 °C. The microhardness of the composite was increased by 75.5 HV, and the corrosion rate improved by 375.36 μAcm^{-2} by the B_4C ratio.

Advanced powder metallurgy techniques are used to process metals by creating objects from fine metallic powders. The process combines the powder form of matrix and reinforcement in specific weight proportions. The powders are compacted into the desired shape and subsequently heated to a temperature marginally under the melting region. This enables the particles to form solid bonds. An advantage of the powder metallurgy process is its efficient dispersion of reinforcement particles. Improved mechanical qualities are a direct outcome of the material's increased homogeneity. Kosedag et al.[34,35] studied the behavior of Al 6061 composites containing SiC, B_4C, and hybrid B_4C/SiC particles under low-speed impact conditions. This investigation employed powder metallurgy techniques alongside finite element analysis to conduct both experimental investigations and computational simulations. The findings indicated that the type of reinforcement, the volume percentage, and the hybridization significantly influenced mechanical performance and impact response. Additionally, you can adjust the matrix to reinforcement ratio, allowing the weight percentage of the reinforcement particles to exceed approximately fifty percent. The powder metallurgy process is complex and necessitates operation within a vacuum-protected environment. Sintering in powder metallurgy involves heating and compacting metal mixed particles at the heat that remains below their melting point. Spark plasma sintering is a notable technique for consolidating powders and is particularly valuable for handling nanomaterials. This technique utilizes a combination of pressure and pulse current to compact the densified powder effectively. A direct pulsed current is passed to a conductive die and the powder sample throughout the procedure, creating an electric field that internally heats the powder[36]. Kosedag et al.[37] examined the behavior of SiC-reinforced Al 6061 composites under repeated low-speed impacts, varying in energy levels and volume fractions. The material exhibited increased resistance to impacts following repeated hits, contributing to its hardening under stress and enhancing its toughness. The quantity of reinforcement and the frequency of impacts contributed to increased difficulty, especially in the affected areas. Kalaimani et al.[38] fabricated the Al-SiC-ZrO_2 hybrid nanocomposite and Al-5wt.%SiC composite by the SPS technique and investigated the wear analysis of the hybrid nanocomposite compared with the Al-5wt.%SiC composite. It has been absorbed that Al-5wt.%SiC enhances the better mechanical properties as compared with the Al-5wt.%SiC-15wt.%ZrO_2 hybrid nanocomposite, proving their 52% maximum mechanical and wear attributes. Yu Hong et al.[39] examined the SiC/Al composites produced by using spark plasma sintering, varying the SiC particle sizes and Al alloy compositions. The composites exhibited a SiC volume ratio of 50% and the optimal physical properties of the 16 µm SiC/6061Al composites were achieved through sintering at 50 MPa for 8 minutes at a temperature of 520 ℃. The bending strength reached a remarkable 649 MPa, while the thermal conductivity stood at an impressive 189 W/(m·K). Additionally, the average CTE exhibited a mere 7.9×10^{-6} K^{-1} within the heat spectrum of 50 -100 °C.

The grain structure and mechanical properties of Al/SiC and Al/B_4C composite were developed by the exciting study. There was a lack of research reports to fabricate the composite through the powder metallurgy process. The spark plasma sintering method used to fabricate the aluminum composite compares these mechanical properties with those of pure aluminum and has not been recorded. This study approaches the SPS method to rectify the challenges of particle size and densification range are the primary reasons for the increase in porosity, which affects the grain structure and mechanical characteristics of the aluminum composite. To solve these challenges by ball milling and optimized sintering temperature with times to rectify the problems. An analysis was conducted for mechanical attributes of Al/SiC and Al/B_4C composites, including density, porosity, SEM, XRD, EDX, microhardness, tensile strength, elongation, and compression strength. This analysis presents findings that highlight the advantageous properties of composites, supporting their development and potential for industrial application.

2. Materials and experimental methods

2.1. Materials

The aluminum metal matrix powder with an APS of 25µm (99.0% pure) and SiC, B_4C with an APS of 25µm (99.5% pure) was used as reinforcement and were purchased from Ultra Nanotech in Bangalore, India. Tables 1-3 show the characteristics of Al, SiC, and B_4C powders, and Figure 1 shows the morphological picture of the original aluminum, SiC, and B_4C powders.

Cite: S. T et al., "Effect of SiC and B·C Reinforcements on the Structural and Mechanical Properties of Aluminum Composites Fabricated by Spark Plasma Sintering". Evergreen, 12 (02) 1322-1335 (2025). https://doi.org/10.5109/7363512.

Table 1: Material composition of pure Aluminum powder

Elements	Mn	Cu	Si	Ti	Cr	Zn	Fe	Al
Wt.	0.0023	0.006	0.030	0.004	0.003	0.05	0.03	99.87

Table 2: Material composition of Silicon carbide powder

Elements	Ba	Al	K	Fe	Ca	Ni	S	Mg	Na	Ti	Si
Wt.	0.05	0.21	0.04	0.23	0.04	0.01	0.03	0.01	0.07	0.02	99.3

Table 3: Material composition of Boron carbide powder

Elements	B_2O_3	O	C	Fe	N	Si	B
Wt.	0.05	0.06	2.5	0.024	0.24	0.012	97.1

Table 4: Composition of the specimens

S. No.	Samples Name	Composition ratio
1	Al	Pure aluminum
2	S1	Al+5%SiC
3	S2	Al+10%SiC
4	S3	Al+15%SiC
5	B1	Al+5%B_4C
6	B2	Al+10%B_4C
7	B3	Al+15%B_4C

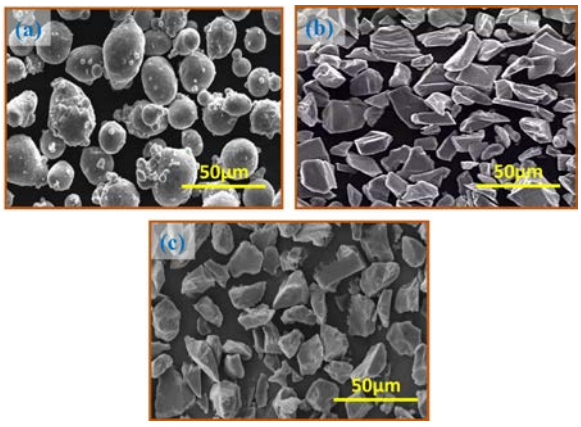

Fig. 1: SEM image of (a) Pure aluminum, Reinforcements, (b) SiC, (c) B_4C

2.2. Experimental Methods

The pure aluminum as a base matrix base was reinforced accompanied by the ceramic particles of SiC & B_4C to synthesize by the spark plasma sintering technique such as Al/SiC and Al/B_4C composite. The composite composition is prepared as followed by Table 4. using the Shimadzu UX820S Precision (0.01g – 820g) weight balance scale. The composition of each sample, marked as A, S1, S2, S3, B1, B2, and B3, was determined by carefully selecting the wt.% of reinforcement particles. The powder mixtures were combined at room temperature
for 60 minutes using a ball mill process by Pulverisette classic line tester, with a milling speed of 200rpm. Five tungsten carbide spheres, each with a diameter of 5 mm, were employed to combine the particles. The collected grinding powder underwent a drying process in a hot dryer set at a specified temperature of 70 °C, and the green compaction method was performed using a hydraulic force of 400 MPa, along with the appropriate mold and die, as shown in Figure 2. The green compaction samples were introduced into the SPS process, the samples were meticulously covered with graphite wrapping paper and then positioned within the graphite mold has a diameter of 25 mm and a height of 40 mm. Stage (1) The vacuum process eliminates moisture, hydrogen, and oxygen gases extracted from the plasma shock chamber mold and punches, followed by Figure 3. After the vacuum process, resistance heat and pressure of 35 MPa are applied in stage (2). Stage (3) introduced the primary sintering process. The pulsed direct current had been released (plasma spark) at 300 °C, with the gaps between particles under pressure during the process of sintering, and the pulsed current diffused throughout the outermost layer of the particles for up to 10 minutes. In the secondary sintering process introduced in stage (4) at the temperature of 550 °C, the necks between the particles eventually form by bonding these molten regions through the electron current present during the ON time, while vacuum generation occurs during the OFF time. In stage (5), the heat was applied to the mold in a series of steps. This allowed partial melting of the aluminum and sealing of the dense air poles through plasma sparks. Increasing plasma heat for 15 minutes with constant pressure during the spark plasma process is recommended to achieve a more effective binding in the grain structure. Stage (6) allows cooling of the specimen to room temperature.

Cite: S. T et al., "Effect of SiC and B·C Reinforcements on the Structural and Mechanical Properties of Aluminum Composites Fabricated by Spark Plasma Sintering". Evergreen, 12 (02) 1322-1335 (2025). https://doi.org/10.5109/7363512.

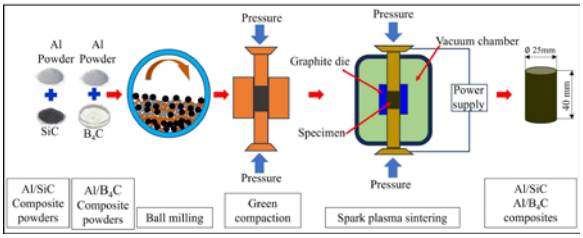

Fig. 2: Spark plasma sintering process

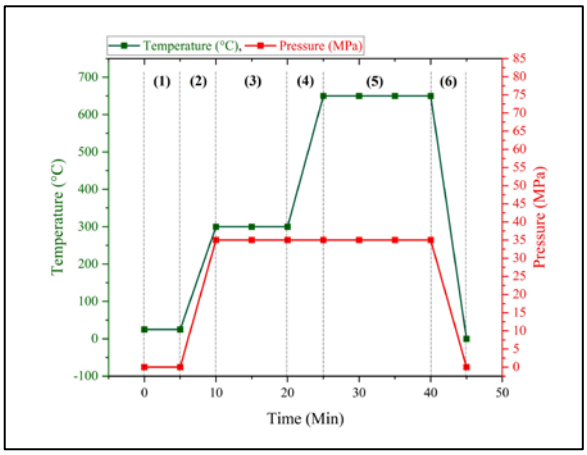

Fig. 3: Temperature and pressure of sintering process

2.3. Materials characterization

2.3.1. Density

The Archimedes principle was applied to the aluminum matrix, and reinforced particles within the specimens were utilized to ascertain their densities. Weighing the sample in air and another fluid with a known density is all that is required for this density measuring technique. The following equation for the density (ρ_{cm}) of the composites may be obtained by using Archimedes' principle:

$$\rho_{cm} = \frac{m_a}{m_a - m_w}\,\rho_w \qquad (1)$$

Where m_a represents the composite sample mass in air, m_w represents the mass of distilled water, and ρ_w represents the density of distilled water 998 kg/m^3 is the density of distilled water at 20 °C. The densities of the composite material and base metal matrix were determined using this technique.

Porosity levels throughout the fabrication of aluminum matrix composite are typically expected due to prolonged particle feeding and increased surface area exposed to air. The porosity volume percentage, size, and distribution in cast CMs significantly impact the regulation of mechanical characteristics. It is essential to minimize porosity levels. Porosity is inevitable in casting, although it may be managed and regulated. The porousness of the composite materials was assessed using the equation (2):

$$Porosity\ (\%) = \frac{\rho_{th} - \rho_{Exp}}{\rho_{th}} \times 100 \qquad (2)$$

Where ρ_{th} denotes the density of the theoretical method and ρ_{Exp} denotes the density of the experimental method, respectively. The theoretical densities ρ_{th} for a single component may be determined using the rule of mixtures by the equation (3).

$$\rho_{th} = \rho_{Al}V_{Al} + \rho_r V_r \qquad (3)$$

Let ρ_{Al} represent the density of the aluminum matrix, V_{Al} denotes the volume ratio of the aluminum matrix, ρ_r indicates the density of reinforcement, and V_r signifies the volume fraction of reinforcement.

2.3.2. EDX analysis

The PANalytical X-Pert Pro equipment was used in order to carry out an X-ray diffraction examination on aluminum composites. Furthermore, samples of Al/SiC and Al/B4C were analyzed. Over a range of 20° to 80° in 2θ, the analytical peak intensities were collected by several measurements.

2.3.3. XRD Analysis

To determine the microcrystalline structure and multiple phases of sintered aluminum composites X-ray diffraction (XRD) analysis utilized a D8 Advance diffractometer from Bruker AXS Inc. based in Madison WI USA. The examination utilized Cu Kα radiation with 1.5406 Å wavelength at an operating power of 40 kV and 40 mA to produce consistent and powerful X-ray illumination. The analysis ranges from 20° to 70° produced X-ray diffraction patterns that enabled the detection of crystalline phases by applying (nλ=2dsinθ) in Bragg's Law. A combination of low step steps at 0.01° together with the slow scanning parameters of 0.02 steps/sec produced high-resolution results which gave distinctive structures about the composite materials.

2.3.4. Hardness strength

The microhardness test determines the hardness of Al/SiC and Al/B$_4$C sample parts. The hardness is evaluated using the Vickers hardness Shimadzu HMV-2 type testing apparatus under ASTM E384 at ambient temperature (25°C)[40]. The Al/SiC sample consists of Al, S1, S2, and S3, whereas the Al/B$_4$C sample consists of Al, B1, B2, and B3. The hardness test was conducted by applying a standardized indentation method and the impression of a specific shape on the surface of the samples, using an applied weight of 500 gf (4.90 N), and maintaining this pressure for 10 seconds. Subsequently, the diagonals (d_1 and d_2) indentation was measured using optical methods, and three indentation tests were performed for each sample. The microhardness value is determined using equations 4 and 5[41]. *HVN* represents the Vicker hardness

number, which is measured in Vicker units. *F* denotes the test load, measured in (gf), and *d* represents the average value of the diagonal length, measured in (mm).

$$HVN = 1854.4 \times \frac{F}{(d^2)} \quad (4)$$

$$d = \frac{d_1 + d_2}{2} \quad (5)$$

2.3.5. Tensile strength

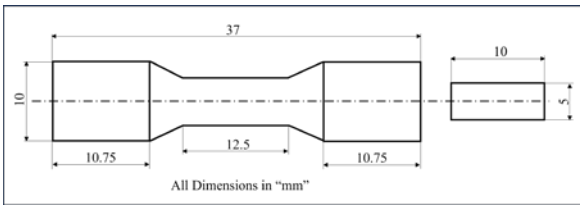

Fig. 4: ASTM standard tensile test sample

The tensile strength evaluation was conducted in a Universal Testing Machine with a capability of 400 kN. The load on the samples was gradually increased by 5 kN. The samples were well mixed. Specimen measurement is shown in Figure 4. The tensile testing was conducted under ASTM Standard E8-82[42]. A crosshead velocity of 2.5 mm/min was used.

2.3.6. Compression strength

In accordance with the ASTM E9 standard pertaining to metallic materials, cylindrical specimens measuring 10 mm in diameter and 40 mm in length were prepared for the compression testing procedure. The testing was conducted using a Universal Testing Machine (UTM) equipped with a 100 kN load cell. The crosshead speed was maintained at 0.5 mm/min to ensure a consistent strain rate during the testing process. All tests were conducted at room temperature, and the recorded Figures for compressive strength were documented for future reference.

3. Result and Discussion

3.1. Microstructure

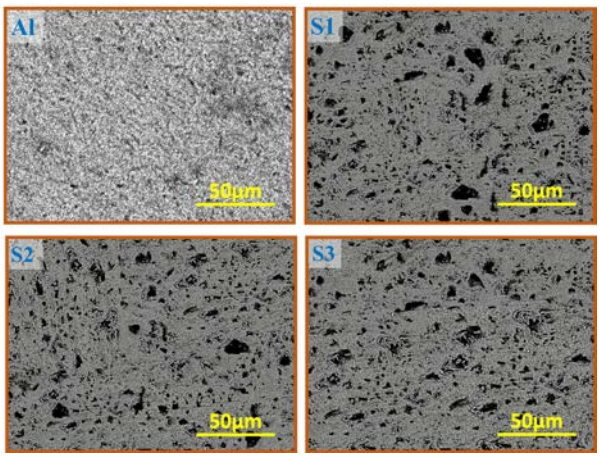

Fig. 5: SEM image of Al/SiC composite samples

Figure 5 presents SEM images illustrating the improvements in the microstructure of Al/SiC composites as the SiC reinforcing content increases. The sample Al depicts the aluminum matrix devoid of any reinforcements. The microstructure exhibits a predominantly homogeneous and dense characteristic, devoid of any visible second-phase particles. In the S1 sample, which consists of 95 wt.% aluminum and 5 wt.% SiC, the SiC particles are sparsely distributed and uniformly dispersed throughout the aluminum matrix. As the SiC concentration in S2 increases to 10 wt.%, there is a significant increase in the number of reinforcement particles. The distribution within the matrix is more uniform, with some degree of particle agglomeration observed. In S3 (Al–85 wt.%, SiC–15 wt.%), an increased presence of SiC particles indicates a higher degree of clustering, resulting in a less continuous matrix. The darker regions represent SiC particles, while the lighter regions correspond to the aluminum matrix. The observed darker regions and increased contrast from S1 to S3 indicate the successful incorporation of SiC. The morphology of the SiC particles remain irregular and is distributed randomly throughout the composites[43]. Additionally, there exist small pores and microvoids that tend to enlarge as the quantity of reinforcement increases. The observed microstructural characteristics indicate an enhanced interaction between particles and the matrix, potentially resulting in improved mechanical properties due to increased reinforcement.

Figure 6 shows the SEM micrographs illustrating Al/B_4C composites containing varying amounts of reinforcement. The Al sample, representing the unreinforced matrix, exhibits a dense and homogeneous structure devoid of any particles from a secondary phase. In B1 (Al–95 wt.%, B_4C–5 wt.%), black areas become visible, evenly distributed throughout the matrix, consisting of B_4C particles. As the concentration of B_4C in sample B2 increases to 10 wt.%, there is a corresponding increase in particle density, accompanied by more pronounced dispersion and the formation of smaller clusters. The B3 sample, comprising 85 wt.% Al and 15 wt.% B_4C, exhibits a higher concentration of B_4C. The distribution of particles is more uniform, resulting in a denser arrangement throughout the matrix. The increased frequency and prominence of the black spots indicate that B_4C has been effectively incorporated into the aluminum matrix[44]. The presence of microvoids and porosities is notable, particularly in samples with a high concentration of B_4C. These features may serve as sites where particles can hold to one another. The microstructure transitions from a base matrix in Al to a reinforced matrix in B3, characterized by a high amount of ceramic particles. The increased volume percentage of B_4C enhances the dispersion of reinforcement and the formation of interfaces, which is expected to influence the mechanical behavior of the composites.

Cite: S. T et al., "Effect of SiC and B·C Reinforcements on the Structural and Mechanical Properties of Aluminum Composites Fabricated by Spark Plasma Sintering". Evergreen, 12 (02) 1322-1335 (2025). https://doi.org/10.5109/7363512.

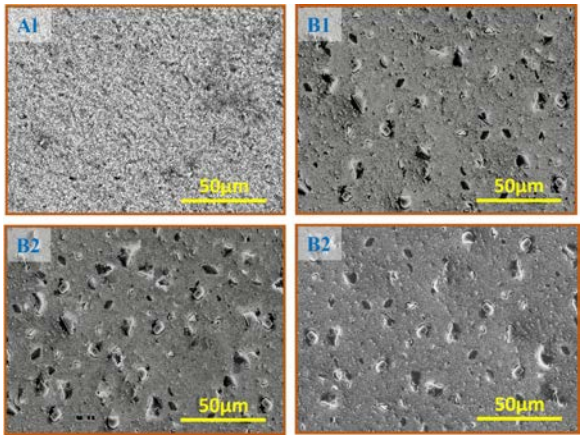

Fig. 6: SEM image of Al/B_4C composite samples

3.2. XRD Analysis

The XRD plot validates the inclusion of aluminum and SiC, as indicated by the distinct peaks in Figure 7. The Al sample peaks observed in pure aluminum (Al) at miller indices 111, 200, 220, and 311 correspond to specific crystallographic planes within the aluminum (JCPDS 85-1327, 65-2869)[45]. The peaks were denoted at the angle of 38.33 °C, 44.47 °C, 65.13 °C and 78.12 °C respectively [46]. The S1, S2, and S3 are reinforced with SiC, and the aluminum exhibits the highest peak, with SiC following closely behind. The Al/SiC particles peak (111) orientation at 35. 81 °C, small peak (220) at 41.56 °C and the average peak (311) at 72.45 °C. The peaks corresponding to aluminum and SiC were identified by referencing JCPDS files (file numbers 040787 and 49-1431, respectively)[47,48]. The XRD pattern confirmed the composite material's aluminum matrix and SiC particulate. The highest intensities of SiC are observable and show a positive correlation with the SiC content. No evidence of new development of phases was observed throughout the sintering process, as no newly formed peaks appeared in any XRD pattern. The fabricated samples have been strengthened with SiC.

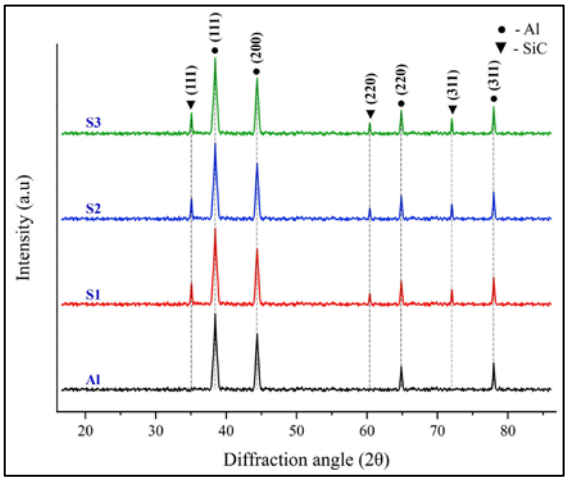

Fig. 7: The X-ray diffraction analysis of Al/SiC composite samples

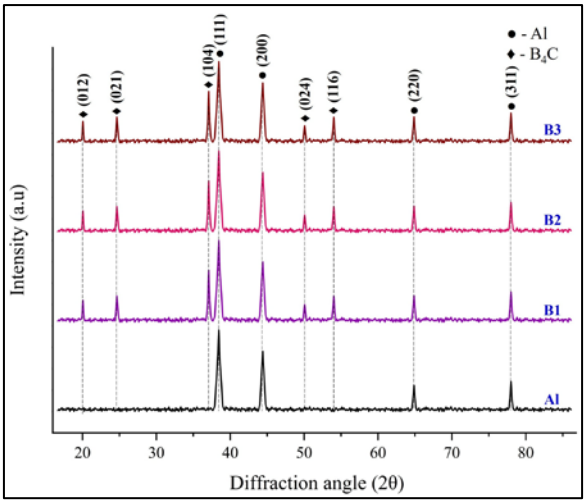

Fig. 8: The X-ray diffraction analysis of Al/B_4C composite samples

The XRD graph confirms the existence of aluminum and B_4C, as evidenced by the unique peaks in Figure 8. The B1, B2, and B3 are reinforced with B_4C, and the aluminum indicates the highest peak, with B_4C particles. The Al/B_4C observed the peaks at (012) at 20.9 °C, (021) at 25.67 °C, (104) at 37.8 °C, (024) at 50.8 °C and (116) at 54.8 °C average peak of B_4C crystal was found, confirming JCPDS (75-0424)[45]. It is clear that the Al-base matrix concentration and peak B_4C intensities strongly correlate.

3.3. Energy Dispersive Spectrum Analysis

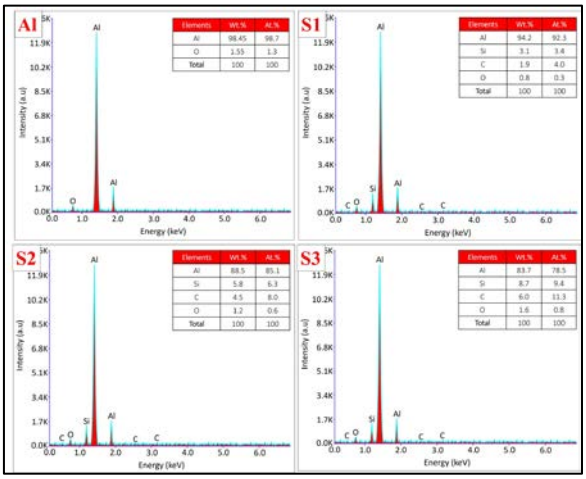

Fig. 9: X-ray diffraction analysis of Al/SiC composites samples

The examination of Al/SiC composite samples utilizing Energy Dispersive X-ray Spectroscopy (EDX)in Figure 9, highlights variations in the amounts of SiC present. The elemental composition of the samples is presented. The analyzed sample of pure aluminum (Al) consists predominantly of aluminum at 98.45 wt.%, with a minor presence of oxide at 1.55 wt.%, indicating a high level of purity. Sample S1 consists of 95% aluminum and 5% silicon carbide (SiC). The analysis indicates that the

aluminum matrix contains a mixture of Si at 3.1 wt.% and C at 1.9 wt.%, suggesting the incorporation of SiC particles. The oxide level remains at a low concentration of 0.8 wt.%, indicating that oxidation is limited. With an increase in SiC content in S2 (Al 90 wt.%, SiC 10 wt.%), the weight percentages of Si and C rise to 5.8 wt.% and 4.5 wt.%, respectively, while the percentage of Al decreases to 88.5 wt.%. This indicates an increase in the reinforcing content. S3, comprising 85 wt.% aluminum and 15 wt.% silicon carbide, exhibits higher concentrations of silicon at 8.7 wt.% and carbon at 6.0 wt.% compared to S2. Conversely, the aluminum content is reduced to 83.7 wt.%. The presence of oxide in all samples, albeit in minimal quantities, may be attributed to surface oxidation processes. The spectra distinctly exhibit peaks corresponding to Al, Si, C, and O, thereby validating the anticipated distribution of elements. The intensity of the peaks for Si and C increases from S1 to S3, which correlates with the increase in SiC concentration. The atomic percentage values correspondingly align with the variations in composition, indicating an increase in Si and C levels as the concentration of SiC escalates. The results indicate that SiC particles were effectively dispersed within the Al matrix, confirming the accuracy of the intended compositions. The results indicate a strong correlation between the matrix and reinforcement phases. This study provides significant compositional evidence that Al/SiC composites can be fabricated and that their structure exhibits strength.

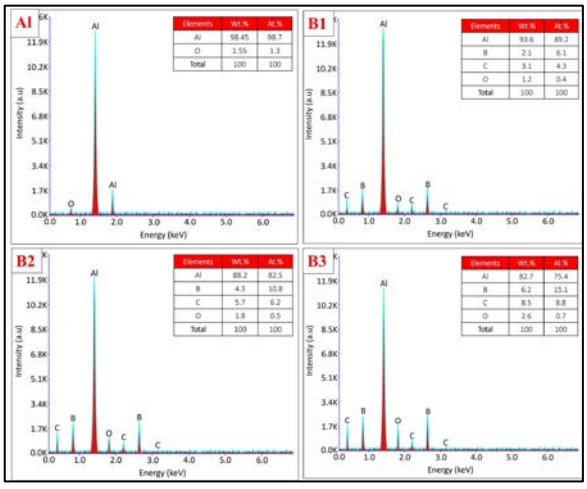

Fig. 10: X-ray diffraction analysis of Al/B4C composite samples

The Energy Dispersive X-ray Spectroscopy (EDX) analysis of Al/B4C composite samples demonstrate the distribution of elements and confirms the successful incorporation of B4C into the aluminum matrix shown in Figure 10. The aluminum sample (Al) exhibits a high purity level, comprising 98.45 wt.% aluminum and a minimal presence of oxide at 1.55 wt.%, indicating its refined state. Sample B1 consisted of 95 wt.% aluminum and 5 wt.% B4C. The addition of boron at 2.1 wt.% and carbon at 3.1 wt.% suggests the incorporation of B4C particles, resulting in a reduction of the aluminum concentration to 93.6 wt.%. The concentrations of boron and carbon in sample B2 (Al 90 wt.%, B4C 10 wt.%) increase to 4.3 wt.% and 5.7 wt.%, respectively, whereas the concentration of aluminum decreases to 88.2 wt.%. Sample B3, comprising 85 weight percent aluminum and 15 weight percent boron carbide, exhibits an increased boron content of 6.2 weight percent and carbon content of 8.5 weight percent, whereas the aluminum content has decreased to 82.7 weight percent[49]. The quantity of oxide present in all samples remains minimal, indicating that only small amounts are detected. The spectra exhibit clear and distinct peaks corresponding to B, C, Al, and O. The intensities of the B and C peaks increase from B1 to B3, consistent with the elevated B4C reinforcement. The atomic percentage data supports the observed compositional trend, particularly highlighting the increasing atomic ratios of B and C. The results indicate that B4C was effectively distributed within the Al matrix, consistent with the intended compositions. The observed ratios of the elements indicate a strong phase interaction between the aluminum and the B4C reinforcement. The EDX results validate the synthesis of the composite and establish a compositional basis for subsequent microstructural and mechanical characterization of the Al/B4C system.

3.4. Density

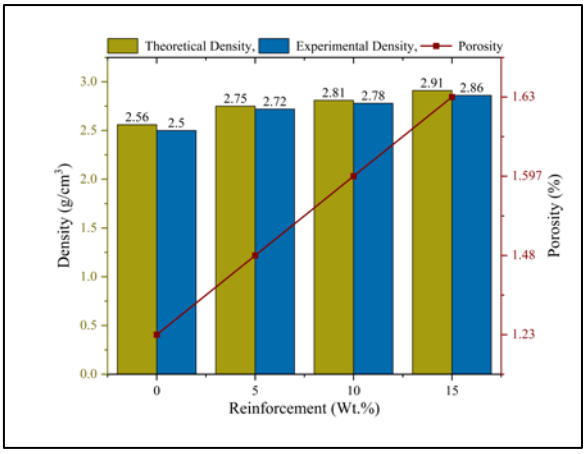

Fig. 11: Al/SiC composite samples density, reinforcement, and porosity

The density of Al/SiC should increase as the SiC content increases because of the high density of SiC carbide compared to Al, as shown in Figure 11. The theoretical density is calculated by equations 1 and 2 for both samples of Al/SiC and Al/B4C. The theoretical density values are greater than the values obtained by experimentation because of the air pores and fluid absorption present in the samples. The experimental density of the Al/SiC

composite was reinforced by the SiC particle by 5, 10, and 15 wt.% with the aluminum base matrix, with the results of S1 being 2.72, S2 being 2.78, and S3 being 2.86 g/cm^3 respectively. By the sintering technique, the samples of Al, S1, S2, and S3 were increased in low-density value, as the difference from Al to S3 was 0.36 g/cm^3.

The sample of Al/B_4C composite reinforced by B_4C particles by 5, 10, and 15 wt.% with aluminum base matrixes by the result of B1 is 2.52, B2 is 2.47, and B3 is 2.41 g/cm^3 respectively, as shown in Figure 12. An increased addition of B_4C would enhance the grain limitations between the two material types[50]. Therefore, an inconsistent combination of Al and B_4C would negatively affect the relative density, resulting in a decreased relative density in the composites upon adding the volume ratio of B_4C [51].

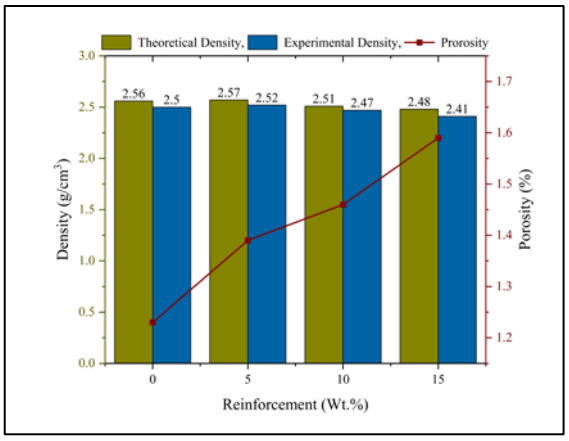

Fig. 12: Al/B_4C Composite samples density, reinforcement, and Porosity

3.5. Microhardness

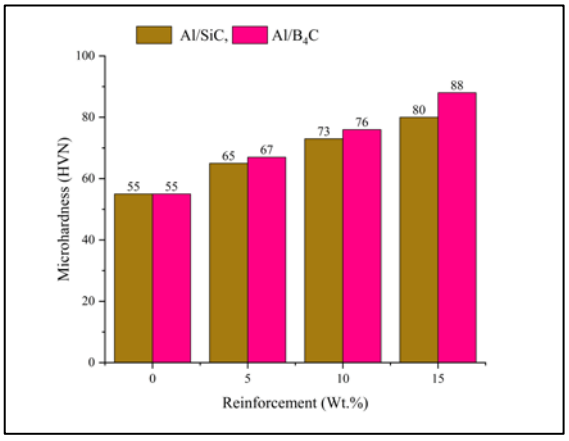

Fig. 13: Microhardness of the Al/SiC and Al/B_4C samples

The microhardness of the sintered Al/SiC samples is illustrated in Figure 13. In this average, pure aluminum (Al) exhibited a microhardness value of 55 HV, while the S1 sample, which is Al with 5% SiC, demonstrated 65 HV. The S2 sample, which is Al with 10% SiC reinforcement, increased the microhardness value to 73 HV, and the S3 sample exhibited a microhardness value of 15%. The addition of SiC resulted in a higher microhardness of 80 HVN. This indicated an increase in the weight percentage of SiC, which enhanced the microhardness value of the aluminum composite containing SiC reinforcement particles within the Al matrix[52]. It was notable for increasing the SiC reinforcement, and the composite material changed the ductile phase to a brittle nature. Subsequently, the Al/B_4C microhardness sintered with the B1 sample, Al composite with 5% B_4C demonstrated a hardness value of 67 HV. The microhardness of the B2 sample, incorporating 10% B_4C reinforcement, was determined to be 76 HV. Similarly, the B3 sample, 15% addition of B_4C, exhibited a maximum microhardness of 88 HVN. The results showed a rise in the B_4C weight percentage, leading to an increase in the microhardness value of the aluminum metal matrix composite. This study is significant as it focuses on enhancing the B_4C reinforcement and investigating the resulting brittle characteristic of the composite material[53]. The hardness of the Al/B_4C samples exhibits a higher performance compared to the Al/SiC samples. The higher density of B_4C reinforcement particles compared to SiC reinforcement particles is the reason for this.

3.6. Tensile strength

A noticeable enhancement in the Al/SiC composite material's tensile strength with pure aluminum is shown in Figure 14. The addition of SiC reinforcement particles increased the ultimate tensile strength. Specifically, S1 increased it to 164.59 MPa, S2 to 194.37 MPa, and 178.36 MPa with 5, 10 and 15 wt% SiC reinforcement particles, respectively. It noted a reduction in elongation, and the elongation of the S3 sample resulted in its breakage[54]. The ultimate tensile strength was increased in the Al/B_4C composite material with increasing B_4C content. The addition of hard ceramic particles improves the mechanical properties mainly by transferring stress from the aluminum base matrix to the B_4C-reinforced particles. The Al/B_4C composite samples B1, B2, and B3 experienced an increase to 168.78 MPa, 210.56 MPa, and 180.26 MPa, respectively, when B_4C was added at 5, 10, and 15 wt.%[55]. Al/B_4C composites exhibited marginally superior tensile strength values compared to Al/SiC across the examined range. The data indicates that the increased hardness and modulus of B_4C may enhance its effectiveness as a reinforcing mechanism. The data indicate that a 10 wt.% reinforcement yields the optimal mechanical performance regarding tensile strength. The findings reveal that integrating ceramic particles into aluminum matrices improves tensile strength. Excessive reinforcement may negatively impact mechanical strength. This study analyzes the importance of achieving an optimal balance between reinforcement content and overall performance in the design of advanced materials.

Cite: S. T et al., "Effect of SiC and B·C Reinforcements on the Structural and Mechanical Properties of Aluminum Composites Fabricated by Spark Plasma Sintering". Evergreen, 12 (02) 1322-1335 (2025). https://doi.org/10.5109/7363512.

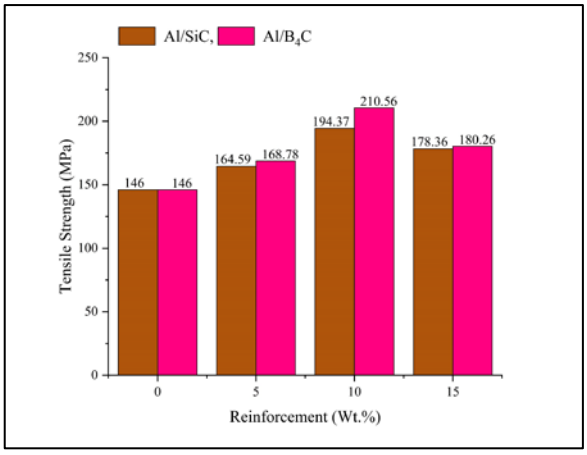

Fig. 14: Tensile strength of the Al/SiC and Al/B4C composite samples

3.7. Elongation strength

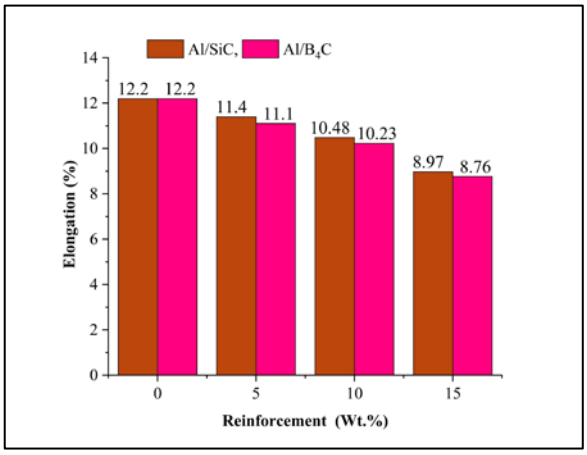

Fig. 15: Elongation strength of the Al/SiC and Al/B4C samples

Figure 15 shows the Al/SiC and Al/B4C composites with varying amounts of reinforcement. The unreinforced aluminum matrix has the maximum elongation of 12.2% for both composites. When ceramic reinforcements are added, both Al/SiC and Al/B4C composites show a steady decline in elongation. The elongation lowers to 11.4% for Al/SiC and 11.1% for Al/B4C when the reinforcement is 5 wt.%. This graph exhibits that the hard particles are initiated to make the material less ductile. When the amount of reinforcement rises to 10 wt.%, the elongation is reduced even further, to 10.48% for Al/SiC and 10.23% for Al/B4C. This drop is because the hard ceramic prevents the particle's dislocation motion, which causes the material to break early when it is under tensile stress. At 15 wt.%, Al/SiC has the lowest elongation value at 8.97% and Al/B4C has the lowest at 8.76%. This finding establishes an inverse relationship between reinforcing content and ductility. The overall direction indicates that increased ceramic content enhances rigidity while simultaneously reducing flexibility. The increased elongation values in Al/SiC composites indicate superior retention of ductility[56] compared to Al/B4C. This advantage may be attributed to the varying shapes of the particles and their distinct binding interactions with the matrix. Minimizing loss in elongation requires an even distribution of reinforcement and strong interfacial bonding. Despite a reduction in ductility levels, the composites remain suitable for structural applications.

3.8. Compression strength

Figure 16 shows the compression strength values for Al/SiC and Al/B4C composites with different amounts of reinforcing weight. At 0 wt.% reinforcement, both composites have the same baseline compression strength of 150 MPa, which is the same as the unreinforced pure aluminum sample. When the amount of reinforcement increased to 5 wt.%, the compression strength raised to 225 MPa for Al/SiC and 223 MPa for Al/B4C. This shows that ceramic particles make the structure stronger. When there is 10% reinforcement, the composites have the highest compression strength: 257 MPa for Al/SiC and 251 MPa for Al/B4C. This improvement is due to the reinforcing particles being better spread out, the material being less likely to distort, and the load is better distributed throughout the matrix. At this stage, Al/SiC demonstrates superior performance compared to the other composite materials. This may be because of the way the particles stick together and fit into the matrix. However, increasing the reinforcement to 15 wt.% causes a small lack in strength, with Al/SiC decreased to 246 MPa[57] and Al/B4C dropping to 238 MPa. This drop might mean that particles are clustering together and that the composite material is becoming more brittle. Both composites exhibit a significant improvement in compression strength relative to the base aluminum matrix at all degrees of reinforcement. This proves that SiC and B4C can be used to strengthen things. The way the material behaves under compression shows that the reinforcement makes it better able to hold up under heavy pressures. At 10 wt.% reinforcement for both kinds, the best qualities are shown. After that, the strengthening effect is significantly lessened. The findings clearly show that adding ceramic particles in a regulated way makes aluminum matrix composites better at handling compression. In general, both SiC and B4C are good reinforcements, but SiC at 10 wt.% gives the strongest results.

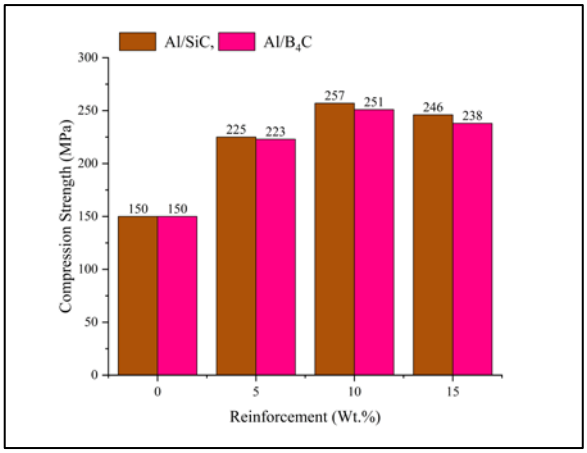

Fig. 16: Compression strength of the Al/SiC and Al/B_4C samples

4. Conclusion

The aluminum base matrix was reinforced with different reinforcement such as SiC and B_4C by a varying range of (5,10 and 15 wt.%) and its fabricated Al/SiC and Al/B_4C as two different composites using the technique of spark plasma sintering. According to the SPS method, particle size and densification range are the primary reasons for the increase in porosity, which affects the mechanical properties of the aluminum-metal matrix composite.

The SEM, XRD, and EDS analyses detected particle distribution, and the well-developed grain structure of the Al-SiC and Al-B_4C composites was fabricated using the SPS technique.

The Al/SiC composite was identified as having a higher density value in the S3 sample of 2.86 g/$cm^{3,}$ and the Al/B_4C composite, with an increase in the volume content of B_4C, the density of the Al/B_4C composites in sample B3 decreased to 2.42 g/cm^3.

The microhardness of the composites Al-SiC and Al-B_4C increased gradually. The Al/B_4C composite hardness increased to 88 HVN compared to the Al/SiC composite, which is 80 HVN.

The tensile and compressive strength of the composite increased with a reinforcement weight of 10 wt.%. However, even when the weight increased by more than 12 wt.% of reinforcement particles, the strength of the composite decreased.

The unreinforced aluminum matrix exhibited an elongation of 12.2% for both Al/SiC and Al/B_4C composites. The addition of 5 wt.% reinforcement resulted in a reduction of elongation of Al/SiC and Al/B_4C of 11.4% and 11.1%; 10 wt.% was 10.48% and 10.23%, and 15 wt.% was 8.97% and 8.76%, respectively. The outcomes indicate that an increase in ceramic content results in a decrease in the ductility and an increase in the brittleness of the composite material. Nevertheless, the composites remain suitable for structural applications due to their increased stiffness.

The findings indicate that the incorporation of SiC and B_4C reinforcements into aluminum matrix composites significantly enhances their compressive strength. The maximum recorded values were 257 MPa for Al/SiC and 251 MPa for Al/B_4C. Subsequent to this phase, a slight reduction in strength is observed as the particles adhere to one another, resulting in increased brittleness. At every level of reinforcement, Al/SiC demonstrates superior performance compared to Al/B_4C. The findings indicate that the incorporation of regulated ceramic reinforcement enhances the strength of aluminum composites, thereby increasing their load-bearing capacity.

References

1) N.K.Bhoi, H. Singh, and S. Pratap, “Developments in the aluminum metal matrix composites reinforced by micro/nano particles--a review,” J. Compos. Mater., 54 (6) 813–833 (2020). doi:https://doi.org/10.1177/0021998319865307.
2) V.Chak, H. Chattopadhyay, and T.L. Dora, “A review on fabrication methods, reinforcements and mechanical properties of aluminum matrix composites,” J. Manuf. Process., 56 1059–1074 (2020). doi:https://doi.org/10.1016/j.jmapro.2020.05.042.
3) S.Li, X. Yue, Q. Li, H. Peng, B. Dong, T. Liu, H. Yang, J. Fan, S. Shu, F. Qiu, and Q. Jiang, “Development and applications of aluminum alloys for aerospace industry,” J. Mater. Res. Technol., 27 944–983 (2023). doi:https://doi.org/10.1016/j.jmrt.2023.09.274.
4) M.Bhong, T.K.H. Khan, K. Devade, B. Vijay Krishna, S. Sura, H.K. Eftikhaar, H. Pal Thethi, and N. Gupta, “Review of composite materials and applications,” Mater. Today Proc., (2023). doi:https://doi.org/10.1016/j.matpr.2023.10.026.
5) J.Li, W. Li, J. Yu, W. Xiao, and H. Xu, “Blast performance of layered charges enveloped by aluminum powder/rubber composites in confined spaces,” Def. Technol., 18 (4) 583–592 (2022). doi:https://doi.org/10.1016/j.dt.2021.03.014.
6) V.S.Egorkin, I.M. Medvedev, S.L. Sinebryukhov, I.E. Vyaliy, A.S. Gnedenkov, K. V Nadaraia, N. V Izotov, D. V Mashtalyar, and S. V Gnedenkov, “Atmospheric and marine corrosion of peo and composite coatings obtained on al-cu-mg aluminum alloy,” Materials (Basel)., 13 (12) (2020). doi:https://doi.org/10.3390/ma13122739.
7) S.Siengchin, “A review on lightweight materials for defence applications: present and future developments,” Def. Technol., 24 1–17 (2023). doi:https://doi.org/10.1016/j.dt.2023.02.025.
8) J.James, A.R. Annamalai, A. Muthuchamy, and C.-P. Jen, “Effect of wettability and uniform distribution of

reinforcement particle on mechanical property (tensile) in aluminum metal matrix composite—a review," Nanomaterials, 11 (9) (2021). doi:https://doi.org/10.3390/nano11092230.

9) D.M.Shinde, P. Sahoo, and J.P. Davim, "Tribological characterization of particulate-reinforced aluminum metal matrix nanocomposites: a review," Adv. Compos. Lett., 29 2633366X20921403 (2020). doi:https://doi.org/10.1177/2633366X20921403.
10) S.Y.Karao¥uglu, S. Karao¥uglu, and ¥.Imgesu Ünal, "Aerospace industry and aluminum metal matrix composites," Int. J. Aviat. Sci. Technol., 2 (02) 73–81 (2021). doi:https://doi.org/10.23890/ijast.vm02is02.0204.
11) Y.Mao, J. Li, A. Vivek, and G.S. Daehn, "High strength impact welding of 7075 Al to a SiC - reinforced aluminum metal matrix composite," Mater. Lett., 303 130549 (2021). doi:https://doi.org/10.1016/j.matlet.2021.130549.
12) M.S.Surya, and S.K. Gugulothu, "Investigations on powder mixed electrical discharge machining of aluminum alloy 7075–4 wt. % TiC in-situ metal matrix composite," Int. J. Interact. Des. Manuf., 17 (1) 299–305 (2023). doi:https://doi.org/10.1007/s12008-022-00895-0.
13) S.P.Dwivedi, S. Sharma, C. Li, Y. Zhang, A. Kumar, R. Singh, S.M. Eldin, and M. Abbas, "Effect of nano-TiO_2 particles addition on dissimilar AA2024 and AA2014 based composite developed by friction stir process technique," J. Mater. Res. Technol., 26 1872–1881 (2023). doi:https://doi.org/10.1016/j.jmrt.2023.07.234.
14) B.Anjaneyulu, G. Nagamalleswara Rao, and K. Prahlada Rao, "Development, mechanical and tribological characterization of Al_2O_3 reinforced ZrO_2 ceramic composites," Mater. Today Proc., 37 584–591 (2021). doi:https://doi.org/10.1016/j.matpr.2020.05.594.
15) S.Caizhi, L. Hui, W. Feng, H. Xudong, H. Wei, and S. Volodymyr, "Study on the microstructure and mechanical properties of ZrB_2/AA6111 particle-reinforced aluminum matrix composites by friction stir processing and heat treatment," Int. J. Met., 18 (1) 457–469 (2024). doi:https://doi.org/10.1007/s40962-023-01029-2.
16) S.P.Dwivedi, and S. Sharma, "Tribological, corrosion, mechanical, and metallurgical behavior of clay and Al_2O_3-reinforced aluminum-based composite material," Proc. Inst. Mech. Eng. Part E J. Process Mech. Eng., 09544089241234433 (2024). doi:https://doi.org/10.1177/09544089241234433.
17) S.P.Dwivedi, "Microstructure and mechanical behaviour of Al/B_4C metal matrix composite," Mater. Today Proc., 25 751–754 (2020). doi:https://doi.org/10.1016/j.matpr.2019.08.244.
18) V.Mohanavel, "Mechanical and microstructural characterization of AA7178-TiB_2 composites," 62 (2) 146–150 (2020). doi:https://doi.org/10.3139/120.111465.
19) I.A.Ibrahim, F.A. Mohamed, and E.J. Lavernia, "Particulate reinforced metal matrix composites — a review," J. Mater. Sci., 26 (5) 1137–1156 (1991). doi:https://doi.org/10.1007/BF00544448.
20) I.M.R.Najjar, A.M. Sadoun, M.A. Elaziz, H. Ahmadian, A. Fathy, and A.M. Kabeel, "Prediction of the tensile properties of ultrafine grained Al–SiC nanocomposites using machine learning," J. Mater. Res. Technol., 24 7666–7682 (2023). doi:https://doi.org/10.1016/j.jmrt.2023.05.035.
21) E.Kosedag, and R. Ekici, "Low-velocity and ballistic impact resistances of particle reinforced metal–matrix composites: an experimental study," J. Compos. Mater., 56 (7) 991–1002 (2022). doi:https://doi.org/10.1177/00219983211068101.
22) A.K. Yadav, and N. Kumar,"Mechanical and thermal behaviour of stir cast sillimanite/red mud/LM25 Al-alloy metal matrix composite," Materialwissenschaft Und Werkstofftechnik, 54(12), 1648–1658, (2023). doi:https://doi.org/10.1002/mawe.202300090.
23) S.Chintada, S.P. Dora, and D. Kare, "Mechanical behavior and metallographic characterization of microwave sintered Al/SiC composite materials – an experimental approach," Silicon, 14 (12) 7341–7352 (2022). doi:https://doi.org/10.1007/s12633-021-01409-5.
24) G.Anbuchezhiyan, B. Mohan, N. Senthilkumar, and R. Pugazhenthi, "Synthesis and characterization of silicon nitride reinforced Al--Mg--Zn alloy composites," Met. Mater. Int., 27 3058–3069 (2021). doi:https://doi.org/10.1007/s12540-020-00906-3.
25) M.A.Alam, H.H. Ya, M. Azeem, P. Bin Hussain, M.S. bin Salit, R. Khan, S. Arif, and A.H. Ansari, "Modelling and optimisation of hardness behaviour of sintered Al/SiC composites using RSM and ANN: a comparative study," J. Mater. Res. Technol., 9 (6) 14036–14050 (2020). doi:https://doi.org/10.1016/j.jmrt.2020.09.087.
26) B.Leszczyńska-Madej, M. Madej, A. Wąsik, and D. Garbiec, "Spark plasma sintering of Al–SiC composites with high SiC content: study of microstructure and tribological properties," Arch. Civ. Mech. Eng., 23 (4) 1–13 (2023). doi:https://doi.org/10.1007/s43452-023-00771-y.
27) A.Brillon, J. Garcia, F. Riallant, C. Garnier, A. Joulain, Y. Lu, and J.-F. Silvain, "Characterization of Al/B_4C composite materials fabricated by powder metallurgy process technique for nuclear applications," J. Nucl. Mater., 565 153724 (2022). doi:https://doi.org/10.1016/j.jnucmat.2022.153724.
28) H.Guo, Z. Zhang, Y. Zhang, Y. Cui, L. Sun, and D.

Chen, “Improving the mechanical properties of B_4C/Al composites by solid-state interfacial reaction,” J. Alloys Compd., 829 154521 (2020). doi:https://doi.org/10.1016/j.jallcom.2020.154521.

29) Z.O.Pehlivanlı, and M. Pul, “Investigation of the effect of B_4C amount and sintering temperature on the thermal properties of the material in al 1070–b4c composites,” Proc. Inst. Mech. Eng. Part L J. Mater. Des. Appl., 235 (12) 2746–2761 (2021). doi:https://doi.org/10.1177/14644207211035520.
30) K.Velavan, B. Mohan, G. Anbuchezhiyan, and N. Senthilkumar, “Implications of SiC/Al_2O_3 reinforced Al-Mg-Zn alloy hybrid nano composites using vacuum sintering method,” Silicon, 1–9 (2021). doi:https://doi.org/10.1007/s12633-020-00928-x.
31) C.Ozay, and O.E. Karlidag, “Hot press sintering effects and wear resistance of the Al-B_4C composite coatings of an AA-2024 alloy,” 63 (12) 1150–1156 (2021). doi:https://doi.org/10.1515/mt-2021-0057.
32) N.Menachery, S. Thomas, B. Deepanraj, and N. Senthilkumar, “Processing of nanoreinforced aluminium hybrid metal matrix composites and the effect of post-heat treatment: a review,” Appl. Nanosci., 13 (6) 4075–4099 (2023). doi:https://doi.org/10.1007/s13204-022-02704-2.
33) E.Ghasali, M. Alizadeh, T. Ebadzadeh, A.H. Pakseresht, and A. Rahbari, “Investigation on microstructural and mechanical properties of B_4C-aluminum matrix composites prepared by microwave sintering,” J. Mater. Res. Technol., 4 (4) 411–415 (2015). doi:https://doi.org/10.1016/j.jmrt.2015.02.005.
34) E.Kosedag, and R. Ekici, “Low-velocity impact performance of B_4C particle-reinforced Al 6061 metal matrix composites,” Mater. Res. Express, 6 (12) 126556 (2019). doi:https://doi.org/10.1088/2053-1591/ab5815.
35) E.Kosedag, and R. Ekici, “Low-velocity impact behaviors of B_4C/SiC hybrid ceramic reinforced al6061 based composites: an experimental and numerical study,” J. Alloys Compd., 1010 177525 (2025). doi:https://doi.org/10.1016/j.jallcom.2024.177525.
36) A.K.Sharma, R. Bhandari, and C. Pinca-Bretotean, “A systematic overview on fabrication aspects and methods of aluminum metal matrix composites,” Mater. Today Proc., 45 4133–4138 (2021). doi:https://doi.org/10.1016/j.matpr.2020.11.899.
37) R.Ekici, E. Kosedag, and M. Demir, “Repeated low-velocity impact responses of SiC particle reinforced Al metal-matrix composites,” Ceram. Int., 48 (4) 5338–5351 (2022). doi:https://doi.org/10.1016/j.ceramint.2021.11.077.
38) M.Kalaimani, and S. Tajudeen, “Investigation of wear performance in zirconium dioxide reinforced aluminum hybrid nano-composites synthesized by the powder metallurgy process,” SAE Tech. Pap., 1–7 (2024). doi:https://doi.org/10.4271/2023-01-5161.
39) Y.Hong, J. Liu, and Y. Wu, “The interface reaction of SiC/Al composites by spark plasma sintering,” J. Alloys Compd., 949 169895 (2023). doi:https://doi.org/10.1016/j.jallcom.2023.169895.
40) S.Tajudeen, and K. M, “Investigation of the microstructure and mechanical properties of an Al/SiC/ZrO_2 hybrid composite by spark plasma sintering technique,” Gazi Univ. J. Sci., 1 (2024). doi:https://doi.org/10.35378/gujs.1348461.
41) A.Uzun, E. Asikuzun, U. Gokmen, and H. Cinici, “Vickers microhardness studies on B_4C reinforced/unreinforced foamable aluminium composites,” Trans. Indian Inst. Met., 71 (2) 327–337 (2018). doi:https://doi.org/10.1007/s12666-017-1163-1.
42) G.Manohar, K.M. Pandey, and S.R. Maity, “Effect of sintering mechanisms on mechanical properties of AA7075/B_4C composite fabricated by powder metallurgy techniques,” Ceram. Int., 47 (11) 15147–15154 (2021). doi:https://doi.org/10.1016/j.ceramint.2021.02.073.
43) Z.Edward Kennedy, and A.I. Raja, “Evaluation of mechanical properties of Al-B_4C and Al-SiC metal matrix composites – a comparison,” Mater. Today Proc., 55 380–383 (2022). doi:https://doi.org/10.1016/j.matpr.2021.08.356.
44) K.S.A.Ali, V. Mohanavel, S.A. Vendan, M. Ravichandran, A. Yadav, M. Gucwa, and J. Winczek, “Mechanical and microstructural characterization of friction stir welded sic and B_4C reinforced aluminium alloy AA6061 metal matrix composites,” Materials (Basel)., 14 (11) 3110 (2021). doi:https://doi.org/10.3390/ma14113110.
45) S.Chand, P. Chandrasekhar, S. Roy, and S. Singh, “Influence of dispersoid content on compressibility, sinterability and mechanical behaviour of B_4C/BN reinforced Al6061 metal matrix hybrid composites fabricated via mechanical alloying,” Met. Mater. Int., 27 (11) 4841–4853 (2021). doi:https://doi.org/10.1007/s12540-020-00739-0.
46) M.B.A.Shuvho, M.A. Chowdhury, M. Kchaou, B.K. Roy, A. Rahman, and M.A. Islam, “Surface characterization and mechanical behavior of aluminum based metal matrix composite reinforced with nano Al_2O_3, SiC, TiO_2 particles,” Chem. Data Collect., 28 100442 (2020). doi:https://doi.org/10.1016/j.cdc.2020.100442.
47) R.Narayanasamy, T. Ramesh, and M. Prabhakar, “Effect of particle size of SiC in aluminium matrix on workability and strain hardening behaviour of P/M composite,” Mater. Sci. Eng. A, 504 (1) 13–23 (2009). doi:https://doi.org/10.1016/j.msea.2008.11.037.

Cite: S. T et al., "Effect of SiC and B·C Reinforcements on the Structural and Mechanical Properties of Aluminum Composites Fabricated by Spark Plasma Sintering". Evergreen, 12 (02) 1322-1335 (2025). https://doi.org/10.5109/7363512.

48) S.Arif, M.T. Alam, T. Aziz, and A.H. Ansari, “Morphological and wear behaviour of new Al-SiCmicro-SiCnano hybrid nanocomposites fabricated through powder metallurgy,” Mater. Res. Express, 5 (4) 46534 (2018). doi:https://doi.org/10.1088/2053-1591/aabcf0.
49) Y.Bayrak, A. Kisasoz, and R. Sezer, “Production and characterization of B_4C content-dependent aluminum matrix composites fabricated via hot pressing,” J. Mater. Eng. Perform., 34 (2) 1607–1618 (2023). doi:https://doi.org/10.1007/s11665-023-09093-9.
50) M.Didwania, L. Singh, A. Pagare, and S. Sharma, “Wear study of Al 6061 hybrid composite reinforced with sic and B_4C microparticles and fabricated by powder metallurgy method,” Evergreen, 11 (4) 3078–3091 (2024). doi:https://doi.org/10.5109/7326946.
51) L.Zhang, Z. Wang, Q. Li, J. Wu, G. Shi, F. Qi, and X. Zhou, “Microtopography and mechanical properties of vacuum hot pressing Al/B_4C composites,” Ceram. Int., 44 (3) 3048–3055 (2018). doi:https://doi.org/10.1016/j.ceramint.2017.11.065.
52) R.Agnihotri, “Mechanical properties of a Al-SiC metal matrix composites fabricated by stir casting route,” Res. Med. Eng. Sci., 2 (5) 178–183 (2017). doi:https://doi.org/10.31031/rmes.2017.02.000549.
53) A. Abebe Emiru, D.K. Sinha, and A. Kumar, “Fabrication and characterization of hybrid aluminium (Al6061) metal matrix composite reinforced with SiC, B_4C and MoS_2 via stir casting”. Inter Metalcast 17, 801–812 (2023). doi:https://doi.org/10.1007/s40962-022-00800-1.
54) X.Zeng, W. Liu, B. Xu, G. Shu, and Q. Li, “Microstructure and mechanical properties of Al-SiC nanocomposites synthesized by surface-modified aluminium powder,” Metals (Basel)., 8 (4) (2018). doi:https://doi.org/10.3390/met8040253.
55) K.L.Meena, D. A. Manna, D. S.S. Banwait, and D. Jaswanti, “An analysis of mechanical properties of the developed Al/SiC-MMC’s,” Am. J. Mech. Eng., 1 (1) 14–19 (2013). doi:https://doi.org/10.12691/ajme-1-1-3.
56) S.P.Dwivedi, M. Maurya, and S.S. Chauhan, “Mechanical, physical and thermal behaviour of SiC and MgO reinforced aluminium based composite material,” Evergreen, 8 (2) 318–327 (2021). doi:https://doi.org/10.5109/4480709.
57) K.D.Salman, “Comparison the physical and mechanical properties of composite materials (Al/SiC and Al/B_4C) produced by powder technology,” J. Eng., 23 (10) 85–96 (2017). doi:https://doi.org/10.31026/j.eng.2017.10.07.